Environmental Science and Pollution Research (2021) 28:42414–42431
https://doi.org/10.1007/s11356-021-13647-6

RESEARCH ARTICLE

Transcriptomic analysis of *Burkholderia cenocepacia* CEIB S5-2 during methyl parathion degradation

Ma. Laura Ortiz-Hernández[1] · Yitzel Gama-Martínez[2] · Maikel Fernández-López[3] · María Luisa Castrejón-Godínez[4] · Sergio Encarnación[5] · Efraín Tovar-Sánchez[6] · Emmanuel Salazar[5] · Alexis Rodríguez[2] · Patricia Mussali-Galante[2]

Received: 18 August 2020 / Accepted: 22 March 2021 / Published online: 4 April 2021

Abstract

Methyl parathion (MP) is a highly toxic organophosphorus pesticide associated with water, soil, and air pollution events. The identification and characterization of microorganisms capable of biodegrading pollutants are an important environmental task for bioremediation of pesticide impacted sites. The strain *Burkholderia cenocepacia* CEIB S5-2 is a bacterium capable of efficiently hydrolyzing MP and biodegrade *p*-nitrophenol (PNP), the main MP hydrolysis product. Due to the high PNP toxicity over microbial living forms, the reports on bacterial PNP biodegradation are scarce. According to the genomic data, the MP- and PNP-degrading ability observed in *B. cenocepacia* CEIB S5-2 is related to the presence of the methyl parathion-degrading gene (*mpd*) and the gene cluster *pnpABA'E1E2FDC*, which include the genes implicated in the PNP degradation. In this work, the transcriptomic analysis of the strain in the presence of MP revealed the differential expression of 257 genes, including all genes implicated in the PNP degradation, as well as a set of genes related to the sensing of environmental changes, the response to stress, and the degradation of aromatic compounds, such as translational regulators, membrane transporters, efflux pumps, and oxidative stress response genes. These findings suggest that these genes play an important role in the defense against toxic effects derived from the MP and PNP exposure. Therefore, *B. cenocepacia* CEIB S5-2 has a great potential for application in pesticide bioremediation approaches due to its biodegradation capabilities and the differential expression of genes for resistance to MP and PNP.

Keywords Biodegradation · Bioremediation · Metabolism · Organophosphate · Pesticide · Xenobiotics · RNA-seq

Introduction

Organophosphate (OP) pesticides are a group of chemicals (phosphoric acid esters) broadly used as insecticides to control pests in agriculture and household due to their wide action spectrum and high effectiveness (Karasali and Maragou, 2016; Sharma et al., 2020). These pesticides cause the irreversible inactivation of the acetylcholinesterase activity (AChE, EC 3.1.1.7), essential for nervous action in insects and vertebrates. Therefore, these chemicals are classified as

Responsible editor: Philipp Gariguess

✉ Alexis Rodríguez
alexis.rodriguez@uaem.mx

✉ Patricia Mussali-Galante
patricia.mussali@uaem.mx

[1] Misión Sustentabilidad México A.C., Priv. Laureles 6, Col. Chamilpa, C.P 62210 Cuernavaca, Morelos, México

[2] Centro de Investigación en Biotecnología, Laboratorio de Investigaciones Ambientales, Universidad Autónoma del Estado de Morelos, Av. Universidad 1001, Col. Chamilpa, C.P. 62209 Cuernavaca, Morelos, México

[3] Centro de Investigación en Dinámica Celular, Universidad Autónoma del Estado de Morelos, Av. Universidad 1001, Col. Chamilpa, C.P 62209 Cuernavaca, Morelos, México

[4] Facultad de Ciencias Biológicas, Universidad Autónoma del Estado de Morelos, Av. Universidad 1001, Col. Chamilpa, C.P 62209 Cuernavaca, Morelos, México

[5] Centro de Ciencias Genómicas, Universidad Nacional Autónoma de México, Av. Universidad s/n, Col. Chamilpa, C.P 62210 Cuernavaca, Morelos, México

[6] Centro de Investigación en Biodiversidad y Conservación, Universidad Autónoma del Estado de Morelos, Av. Universidad 1001, Col. Chamilpa, C.P 62209 Cuernavaca, Morelos, México

highly toxic. As a consequence of the intensive usage of OP pesticides, several environmental pollution events in agricultural soils and water bodies have been reported (Fosu-Mensah et al., 2016; Okoli et al., 2017). The environmental accumulation of such toxic chemicals is recognized as a menace for fauna (Siddiqa et al., 2016; Dorneles et al., 2017; Poirier et al., 2018) and human health (Upadhayay et al., 2020; Nicolopoulou-Stamati et al., 2016; Jokanović, 2018).

However, even though the use of OP pesticides has been banned in several countries due to their toxicity, some of them, especially parathion and methyl parathion (MP), continue to be widely used for pest control in crops like cotton, rice, bean, and corn, among others (Urióstegui-Acosta et al., 2020). Due to its high toxicity to mammals and the environmental concern associated with the accumulation of OP pesticide wastes in soil, water supplies, and food, it is necessary to develop reliable and economic strategies for OP pesticides detoxification, and elimination (Mulla et al., 2020; Pailan et al., 2020). Microbial biodegradation of pesticides has received particular attention; different bacterial strains capable of biodegrading OP pesticides have been isolated from agricultural soils from different regions worldwide.

Bacterial biodegradation of OP pesticides is related to the activity of enzymes that catalyze the hydrolysis of phosphoester bonds (Bhatt et al., 2021). Among the most studied OP pesticide-hydrolyzing enzymes are phosphotriesterases, as the organophosphorus hydrolase (OPH) encoded in the *opd* (organophosphate-degrading) gene in *Flavobacterium* ATCC 27551 (Mulbry and Karns, 1989), the coroxon hydrolase (HOCA) coded by the gene *hoc*A (coroxon hydrolysis) in *Pseudomonas moteilli* (Horne et al., 2002), and methyl parathion hydrolase (MPH) coded by the gene *mpd* (methyl parathion-degrading) in *Plesiomonas* sp. strain M6 (Zhongli et al., 2001).

Most of the bacteria capable of hydrolyzing MP express the enzyme methyl parathion hydrolase (MPH EC 3.1.8.1.), a triesterase coded in the *mpd* gene. This enzyme catalyzes the hydrolysis of the phosphotriester bond of the MP, releasing *p*-Nitrophenol (PNP) and dimethyl-thiophosphoric acid. These metabolites are not toxic to the nervous system because they are unable to inhibit the AChE activity (Siddavattam et al., 2003; Pakala et al., 2007; Popoca-Ursino et al., 2017). However, PNP is a chemical compound considered an environmental pollutant due to its high toxicity over soil microbiota (Megharaj et al., 1991; Subashchandrabose et al., 2012).

Several bacteria can hydrolyze MP (Kulkarni and Chaudhari, 2006; Zhang et al., 2009a; Zheng et al., 2009; Min et al., 2017; Zhang et al., 2018). However, reports on bacteria capable of efficiently degrading PNP are scarce. Bacterial-mediated degradation of PNP has been studied, reporting two metabolic pathways. The first, denominated as the hydroquinone pathway (HQ), has been reported in Gram-negative bacteria as *Moraxella* sp. (Spain and Gibson 1991), while the second, the hydroxyquinol or benzenetriol pathway (BT), has been reported in Gram-positive bacteria as *Arthrobacter* sp. (Jain et al., 1994) and *Rhodococcus opacus* SAO101 (Kitagawa et al., 2004). The presence of both PNP biodegradation pathways has also been reported in some Gram-negative bacteria, as *Burkholderia* sp. SJ98 (Vikram et al., 2013), *Burkholderia zhejiangensis* CEIB S4-3 (Castrejón-Godínez et al., 2019), and *Pseudomonas* sp. WBC-3 (Zhang et al., 2009b). In these strains, the catabolic genes that encode the enzymes related to PNP degradation (monooxygenases, dioxygenases, reductases, and dehydrogenases) are organized as a gene cluster.

The bacterial strain *Burkholderia cenocepacia* CEIB S5-2 was characterized with the capability of hydrolyzing MP and degrading PNP completely (Fernández-López et al., 2017). The analysis of its draft genome reveals the presence of a cluster of genes (*pnp*ABA'E1E2FDC) related to both known degrading PNP pathways (Martínez-Ocampo et al., 2016). Evaluation of gene expression levels and transcriptional regulation in *B. cenocepacia* CEIB S5-2 may conduct a better understanding of the bacterial response to the presence of both compounds MP and PNP and the biological processes involved in their biodegradation. The present study aimed to evaluate the transcriptional changes generated by the exposure to MP on the bacterial strain *B. cenocepacia* CEIB S5-2, as well as the differential expression of genes related to the hydrolysis of MP and the biodegradation of PNP, through the transcriptome analysis generated by the next-generation sequencing technology RNA-seq.

Materials and methods

Bacterial strain

B. cenocepacia CEIB S5-2 was previously isolated from agricultural soils from the state of Morelos, Mexico. This strain can efficiently hydrolyze the pesticide MP and degrade its main hydrolysis product PNP (Fernández-López et al., 2017); its genome has a total length of around 8,976,170 bp and a G + C content of 65.7%. The PNP degradation profile of this strain was correlated to the presence of a catabolic cluster denominated *pnpABA E1E2FDC* (Martínez-Ocampo et al., 2016).

Chemical reagents

Methyl parathion (*O,O-dimethyl O-4-nitrophenyl phosphorothioate*) analytical grade (99% purity) was purchased from Chem Service Inc. (West Chester, PA, USA). Pesticide working solution (10,000 mg/L) used in all experiments was prepared using HPLC-grade methanol (Merck, Darmstadt, DEU) as solvent.

Culture media, pre-inoculum, and bacterial growth conditions

For the maintenance of the strain and the production of the pre-inoculum of the *B. cenocepacia* CEIB S5-2 for subsequent transcriptomic experiments, three 250-mL independent cultures were incubated (30 °C, 150 rpm) for 12 h using tripticasein soy broth (Bioxon, Becton Dickinson, Mexico State, Mexico), to reach an optical density ($OD_{600\ nm}$) of 1.0. Subsequently, the cell pellet from each culture was collected by centrifugation at 10,000 rpm (4 °C, 10 min) and washed three times with mineral salts medium (MSM), with the following composition in g/L, 2.92 of K_2HPO_4; 0.20 of KH_2PO_4; 2.0 of $MgSO_4{\cdot}7H_2O$; 0.99 of KNO_3; and 0.99 of $(NH_4)_2SO_4$; and after sterilization, 2 mL of trace elements solution (pH 7.00 ± 0.05) composed in g/L by 2.8 of H_3BO_3; 2.55 of $MnSO_4.H_2O$; 0.20 of $CuSO_4.5H_2O$; 2.43 of $CoCl_2.6H_2O$; and 0.25 of $ZnSO_4{\cdot}7H_2O$. Finally, the cell pellets were resuspended in 5 mL of MSM, and the resulting cellular suspension was used for the inoculation of the experimental cultures.

Growth kinetics in the presence of MP were performed to establish adequate sampling points for RNA extraction for subsequent transcriptome sequencing (Fig. 1). Sampling times were selected according to the following considerations; the sampling time 0 h was selected due to the fast MP hydrolysis observed at the beginning of the growth kinetics. The sampling time of 2 h corresponded to the highest PNP concentration observed over the growth kinetics. Finally, the sampling time of 5 h was selected due to the important decreasing in the PNP concentration observed compared to the sampling time of 2 h, thus indicating the biodegradation of this metabolite by the strain.

In the experimental cultures, *B. cenocepacia* CEIB S5-2 (OD_{600nm} = 0.5) was grown in 250 mL Erlenmeyer flasks (30 °C, 120 rpm, 5 h) containing 50 mL of previously sterilized MSM according to Fernández-López et al. (2017). Eighteen culture flasks were inoculated with the strain, nine culture flask were supplemented with 50 mg/L of MP (pesticide exposed condition), and nine without the pesticide (control condition). In the cultures of both experimental conditions, bacterial growth was followed through the OD at 600 nm record, while the release of PNP, resulting from the MP hydrolysis, was followed through the absorbance at 410 nm. At each sampling time (0, 2, and 5 h), the cells of three culture flask were collected by centrifugation (3500 rpm, 4 °C, 10 min) in the presence of 400 μL of RNAlater® (Ambion, Foster City, CA, USA) solution. The obtained cellular pellets were stored at − 70 °C for subsequent ARN extraction.

RNA extraction

Total RNA extraction of each sample was performed according to the TRIzol-chloroform method, following the TRI Reagent® Kit (Sigma-Aldrich, Sheboygan Falls, WI, USA) protocol. Per each sample, an amount of 30 μg of total RNA was processed with 5 μL of DNaseI enzyme solution (Thermo Scientific, Waltham, MA, USA) to eliminate DNA debris remaining in the samples. Subsequently, samples were cleaned and concentrated using "RNA Clean and Concentrator™" columns (Zymo Research, Irvine, CA, USA). Finally, the purified total RNA concentration from each sample (5 μL) was determined according to its absorbance at 260 nm in a Nanodrop 200c (Thermo Scientific, Waltham, MA, USA), while the RNA integrity was evaluated by electrophoresis in 1% agarose gels. Subsequently, the samples were sent to the GENEWIZ company (https://www.genewiz.com/) (South Plainfield, NJ, USA) for quality evaluation, ribosomal RNA elimination, construction of the cDNA libraries, and transcriptome sequencing through the Illumina HiSeq 2 × 150 bp 2000 System (RNA-seq). The quality and concentration of the samples were evaluated by fluorescence

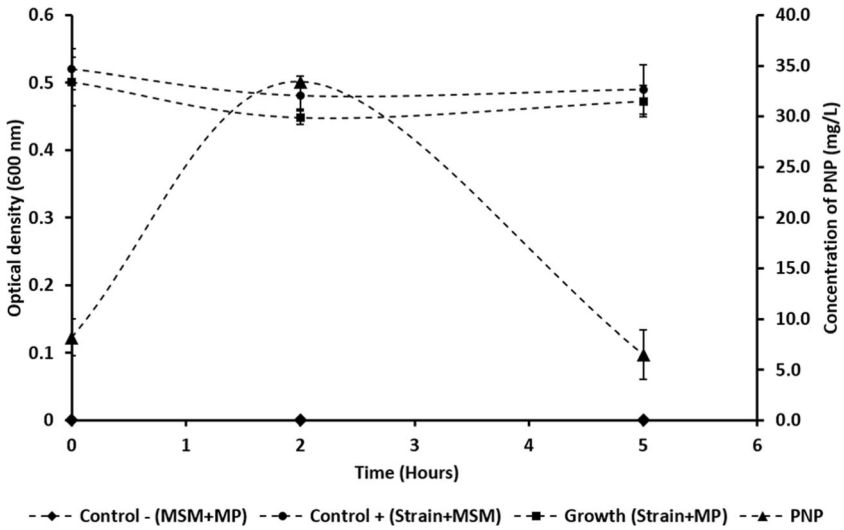

Fig. 1 Hydrolysis of MP and degradation of PNP by *B. cenocepacia* S5-2

(QubitTM), and the integrity of the samples was evaluated by capillary electrophoresis (Agilent 2100 Bioanalyzer). In this method, the resulting electropherogram provides the RNA integrity number (RIN), a numerical index ranging from 1 to 10, where the minimum acceptable value is 8 and a value of 10 indicates that the RNA sample has the highest integrity (Schroeder et al., 2006).

Analysis and mapping of RNA-seq data

The RNA-seq transcriptomic data were processed using the FastQC software (Babraham, Bioinformatics, UK) to get the quality values of the sequences. Subsequently, sequences were processed in the software Cutadapt 2.9 (Martin, 2011) to eliminate the adapters and carried out the low-quality sequences filtering. After processing, the sequences were aligned against the *B. cenocepacia* CEIB S5-2 draft genome (GenBank, LNCR00000000), as the reference genome, using the CLC Genomics Workbench v. 10.0.1 server (Qiagen, Hilden, DEU) for inference of the expressed transcripts; alignments were visualized in the IGV software (Broad Institute, CA, USA) according to Thorvaldsdóttir et al. (2013). The normalization of the obtained readings for the differential expression analysis between both conditions was performed using the DeSeq2 method (Love et al., 2014). Differentially expressed genes (DEGs) were defined as those that showed Log_2 (fold-change) values ≥ 1.5 between both conditions and a *p*-value ≤ 0.05. A principal component analysis (PCA) was performed under PAST version 4.03 software (Hammer et al., 2001) to evaluate the ordination of the samples over sampling times (0, 2, and 5 h) according to their expression profiles in both experimental conditions WMP and MP. This analysis was performed using the log of normalized data corresponding to the 467 genes identified with differential expression (fold-change value ≥ 1.5 and $p \leq 0.05$).

Functional classification

To identify the corresponding assigned function for the DEGs identified and the metabolic process, which they are implicated, an analysis in the Kyoto Encyclopedia of Genes and Genomes (KEGG) pathway color was performed (http://www.genome.jp/kegg/tool/map_pathway2.html). The identification of orthologous (KO, KEGG Orthology) for the *B. cenocepacia* CEIB S5-2 DEGs was performed in the Integrated Microbial Genomes an Microbiomes database (JGI, IMG/M) (https://img.jgi.doe.gov). The respective KO gene functions were assigned using as reference the metabolic pathways dataset of *Burkholderia* sp. RPE67 (Takeshita et al., 2014) in the KEGG database.

DEGs' classification by clusters of orthologous groups (COG)

For the evaluation of the functional categories corresponding to the identified DEGs, a cluster analysis of orthologous groups (COGs) of proteins was performed using the gene database of *B. cenocepacia* CEIB S5-2 from the IMG/M database. The DEGs with a minimum fold-change value of 1.5 and $p < 0.05$ were classified into functional categories (Galperin et al., 2014).

qRT-PCR analyses

For evaluating the transcriptional expression of the set of genes involved in the MP hydrolysis and the degradation of PNP, qRT-PCR analyses were performed. cDNA libraries were synthesized for each sampling time (0, 2, and 5 h) and experimental condition. cDNA libraries synthesis was carried out from 2 μg of the total RNA, previously treated with DNaseI, using the RevertAid H Minus First Strand cDNA Synthesis Kit (Thermo Scientific, Waltham, MA, USA). Each qRT-PCR reaction was carried out in biological and technical triplicates. The cDNA of each sample was used for the transcriptional expression analysis of the interest genes (*mpd* and *pnpABA'E1E2FDC*) between experimental conditions. The RNA polymerase sigma factor 70 (*rpoD*) gene was used as the endogenous expression control due to its constitutive expression. Subsequently, the expression levels of the selected genes were calculated through the $2^{-\Delta\Delta C}{}_T$ method (Livak and Schmittgen, 2001). The primers used for qRT-PCR gene validation were taken from Castrejón-Godínez et al. (2019) and are shown in Table S1. The data have equal sample sizes, and each group presents a normal distribution according to Shapiro–Wilk statistical test (W test). In addition, the Levene test showed homogeneity of variances (Levene test). Therefore, we proceeded to perform a one-way analysis of variance. Subsequently, to compare between pairs of averages, a post hoc Tukey test was performed ($p < 0.05$) (Zar, 2010). Average ± standard deviation and one-way analysis of variance were used to evaluate the effect of the sampling time (0, 2, and 5 h) on relative gene expression ($2^{-\Delta\Delta C}{}_T$).

Experimental determination of the operon organization of the cluster *pnpABA'E1E2FDC*

For the experimental determination of the possible organization of the *pnpABA'E1E2FDC* gene cluster as an operon, PCR reactions were performed using the cDNA library synthesized from the *B. cenocepacia* CEIB S5-2 RNA extracted 2 h post-culture inoculation in the presence and absence of the pesticide MP. For PCR reaction, the following oligonucleotide pairs were employed, *pnpAf-pnpBr*, *pnpE2f-pnpE1r*, *pnpE1f-pnpFr*, *pnpFf-pnpDr*, and *pnpCf-fdxDr*; this set of

oligonucleotides were used to amplify adjacent and overlapping sequences in the gene cluster to determine the possible operon arrangement of the genes related with the PNP degradation and to evaluate differences in the expression levels of these genes between the two experimental conditions. The PCR products were evaluated in 1.5% agarose gels, using *B. cenocepacia* CEIB S5-2 genomic DNA as the positive control and total RNA as the negative control.

Results

B. cenocepacia CEIB S5-2 growth and PNP degradation kinetics

Growth and MP degradation kinetics were performed in MSM supplemented with 50 mg/L of MP. As observed in Fig. 1, at the beginning of the kinetics (0 h), MP is fast hydrolyzed by *B. cenocepacia* CEIB S5-2, releasing PNP in the culture (8.2 mg/L). After 2 h of culture, the PNP concentration reached its higher value in the kinetics (33.4 mg/L); subsequently, the PNP concentration starts to decrease. Finally, after 5 incubation hours, the PNP concentration in the culture diminished to 6.5 mg/L. On the other hand, the PNP release causes slight adverse effects over the bacterial population, mainly after 2 h of culture when the highest PNP concentration was also observed in the culture. Finally, after 5 incubation hours, a slight increase in DO_{600nm} was observed. This finding suggests that *B. cenocepacia* CEIB S5-2 not only can efficiently degrade the PNP, but also it could use the PNP as a carbon source.

Total RNA extraction, yield, and quality

After the total RNA extraction and the treatment of the samples with DNaseI, the total RNA concentration in the samples ranged from 500 to 2500 ng/μL (Table S2). After evaluating the quality, concentration, and integrity of the samples, most of the samples showed acceptable RIN values (Fig. S1), being 6.8 the lowest value, corresponding to the second replicate of the experimental condition with MP at time 5 h (14 Bc T5 R2 WMP), and the highest value 8.9, corresponding to the second replicate of the control condition at time 0 h (5 Bc T0 R2 MP).

Gene expression analysis

The fold-change analysis allowed the identification of the set of genes that showed a differential expression for each sampling time in both experimental conditions, in the absence of pesticide (WMP) as well as in the presence of 50 mg/L of MP. At the initial time (T0) in the control condition without pesticide, no DEGs were observed (Fig. 2). However, in the same condition, at sampling time 2 h, 90 DEGs were observed, while at sampling time of 2 h, 143 genes showed differential expression. Of the DEGs identified, 67 (31.9%) were exclusive of the sampling time of 2 h, and 120 DEGs (57.1%) were observed exclusively in the sampling time of 5 h. Twenty-three DEGs were shared between these two sampling times.

On the other hand, in the experimental condition in the presence of pesticide, at the beginning of the kinetics (T0), seven DEGs were observed; the numbers of differentially expressed genes increased with time; at the sampling time of 2 h (T2), 166 genes showed differential expression, while at 5 h (T5), 232 DEGs were observed. All DEGs observed at T0 were shared with the subsequent sampling times, and 141 DEGs were shared between the sampling times 2 and 5 h. The highest number of exclusive DEGs was observed in the sampling time of 5 h, 91 DEGs (35.4%). Meanwhile, at sampling time T2, only 25 exclusive DEGs (9.7%) were observed. In the presence of MP, several of the identified DEGs encode hypothetical or unknown function proteins. None of the DEGs identified were shared between control and MP-exposed condition, thus indicating that *B. cenocepacia* CEIB S5-2 responds in a differential way to the stress generated by the absence of a carbon source in the control condition and the generated by the exposure to the pesticide MP. Table S3 shows some examples of the DEGs identified in the different sampling times in the strain *B. cenocepacia* CEIB S5-2.

Principal component analyses

In general, the principal component analysis (PCA) separated the sampling time per treatment (MP and WMP). In sampling time of 0 h, the PCA explained 99.97% of the variation in the first two components. In the principal component 1 (PC1), which explained 98.50% of the variation, the genes that encoded for *p*-nitrophenol 4-monooxygenase (*pnp*A) and the hydroxyquinol 1,2-dioxygenase (*pnp*E1/E2) were highly correlated. The genes of the histidine kinase GAF domain-containing protein and a transcriptional regulator of the TetR family showed the highest correlations with the principal component 2 (PC2) which explained 1.46% of the variation (Fig. 3a). In sampling time of 2 h (Fig. 3b), the PC1 explained 69.63% of the variation; the negatively correlated genes were two transcriptional regulators of the TetR family, and the gene of a universal stress protein and the positively correlated genes were those who encode proteins related with the cell motility as the flagellar basal-body rod protein (FlgC), the flagellar basal-body rod modification protein (FlgD), and the flagellar basal-body rod protein (FlgF). The PC2 at T2 explained the 20.95% of the variation. The negatively correlated genes were the outer membrane protein (porin) gene and the gene that encodes the glutaryl-CoA dehydrogenase enzyme. In contrast, the positively correlated genes were a transcriptional regulator, the TetR family, a universal stress protein, and the gene of the (R,R)-butanediol dehydrogenase/meso-butanediol dehydrogenase/diacetyl reductase; the two components have

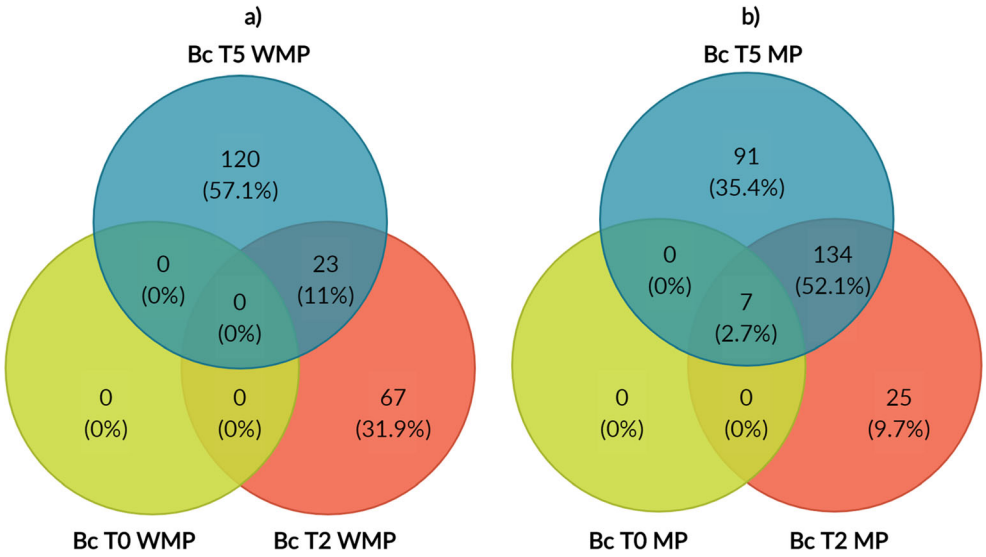

Fig. 2 Venn diagram showing the distribution of differentially expressed genes detected by DESeq2 from each time and genes shared between the three times of each condition. a Genes expressed in the absence of MP and b genes expressed in the presence of MP. No genes shared between conditions were found. Bc, *Burkholderia cenocepacia* CEIB S5-2; T0, time zero h; T2, time 2 h; T5, time 5 h. WMP, without methyl parathion; MP, methyl parathion

an accumulative correlation of 90.58%. Finally, at 5 h sampling time (Fig. 3c), the PCA analysis explained 97.73% of the variation in the two components. The PC1 explained 89.24% of the variation; the genes positively correlated were the 2-polyprenyl-6-methoxyphenol hydroxylase gene, a gene that encodes alcohol dehydrogenase, class IV, the ferredoxin subunit of nitrite reductase, or a ring-hydroxylating dioxygenase gene. The PC2 explained only 8.49% of the variation; the genes negatively correlated were a BON domain-containing protein gene, the histidine kinase GAF domain-containing protein, and a signal transduction histidine kinase gene. In contrast, the genes positively correlated were the uroporphyrinogen-III C-methyltransferase gene, the sulfate adenylyltransferase subunit 1 gene, and a gene that encodes a hypothetical protein.

Identification of COGs

Figure 4 shows the DEGs identified for each sampling time and experimental condition which were classified according to their functional category, with the help of the cluster of orthologous group (COG) database (Galperin et al., 2014). At the initial time (T0) in the control condition, no gene showed a significant differential expression. Subsequently, at the sampling time of 2 h, of the 90 DEGs identified, 24 (26.7%) genes couldn't be associated with a COG; six genes were grouped into poorly characterized categories, four (4.4%) genes in [S] function unknown, and two (2.2%) in [R] general function prediction only. Most of the remaining 60 DEGs identified in T2 were grouped in the following COGs: (1) cell motility [N] with 25 genes (27.8%); (2) amino acid transport and metabolism [E] with seven genes (7.8%); energy production and conversion [C] with six genes (6.7%); cell wall/membrane/envelope biogenesis [M]; and inorganic ion transport and metabolism [P] with four genes (4.4%) each. Meanwhile, in the sampling time of 5 h, 143 DEGs were identified; of these, 52 (36.4%) weren't grouped in a COG; 14 genes were grouped into poorly characterized categories, eight (5.6%) genes in [S] function unknown, and six (4.2%) in [R] general function prediction only. Most of the remaining 77 genes identified in T5 were grouped in the following COGs: (1) carbohydrate transport and metabolism [G] with 19 genes

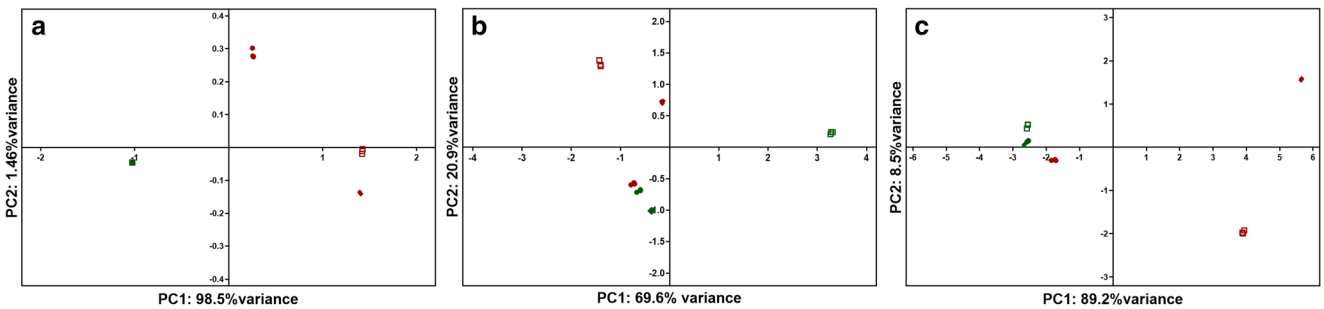

Fig. 3 Principal component analysis of RNA-Seq data. Data corresponding to the control condition are shown in green (T0 filled circles, T2 open squares, and T5 filled diamonds), while data corresponding to the experimental condition with 50 mg/L of MP are shown in red (T0 filled circles, T2 open squares, and T5 filled diamonds). The PCA analyses were performed using normalized RNA-Seq data of a set of 467 with differential expression (fold-change value ≥ 1.5 and $p \leq 0.05$)

(13.3%); (2) inorganic ion transport and metabolism [P] with ten genes (7%); (3) lipid transport and metabolism [I] with eight genes (5.6%); (4) amino acid transport and metabolism [E] with seven genes (5%); (5) energy production and conversion [C] with six genes (4.2%); and (6) cell wall/membrane/envelope biogenesis [M] with six genes (4.2%).

In the presence of MP, at the initial sampling time (T0), 7 DEGs were observed, four (57.1%) of these genes weren't associated to COGs, and the remaining three genes were grouped into an equal number of COGs: (1) transcription [K], (2) transport and metabolism of carbohydrates [G], and (3) transport and metabolism of coenzymes [H]. After 2 h of culture, 166 DEGs were identified, and 57 of these genes (34.3%) weren't associated with a COG, while 15 of the DEGs were grouped in general function prediction only [R] and six in function unknown [S] categories. For the remaining 88 DEGs, the five principal functional categories identified were (1) production and conservation of energy [C] with 16 genes (9.6%); (2) transcription [K] with 13 genes (7.8%); (3) transport and metabolism of coenzymes [H] with 10 genes (6%); (4) carbohydrate transport and metabolism [G] with 9 genes (5.4%); and (5) inorganic ion transport and metabolism [P] with 8 genes (4.8%). At the sampling time of 5 h, of the 232 DEGs, 73 weren't grouped into a COG, while 15 of the DEGs were grouped in the general function prediction only [R] and nine in function unknown [S] categories. The main functional categories that group the remaining 136 DEGs were (1) energy production and conversion [C] with 21 genes (9.05%); (2) inorganic ion transport and metabolism [P] with 18 genes (7.76%); (3) carbohydrate transport and metabolism [G] with 17 genes (7.33%); (4) transcription [K] with 17 genes (7.33%); and (5) transport and metabolism of coenzymes [H] with 11 genes (4.74%).

Functional annotation by Kyoto Encyclopedia of Genes and Genomes (KEGG)

The DEGs identified in both conditions were submitted to an analysis in the KEGG database (Ogata et al., 1999), using the genome of the strain *Burkholderia* sp. RPE67 (Takeshita et al., 2014) as reference. In the absence of the pesticide, 53 of 90 DEGs identified at the sampling time of 2 h (59%) were located in metabolic pathways by KEGG; the exclusive metabolic pathways in T2 were (1) ABC transporters, (2) methane metabolism, (3) biosynthesis of antibiotics, and (4) biosynthesis of amino acids. While in the sampling time of 5 h, 54 of the 143 DEGs identified (38%) were located in metabolic pathways by KEGG. In this sampling time, the exclusive metabolic pathways identified were (1) carbon fixation in photosynthetic organisms, (2) pentose phosphate pathway, (3) methane metabolism, and (4) starch and sucrose metabolism (Fig. 5).

In the presence of MP, at the initial time (T0), through the analysis in the KEGG database, only one DEG was located in a metabolic pathway related to the degradation of aromatic compounds. After 2 h of culture (T2), 53 of the 166 DEGs identified were located in metabolic pathways in KEEG. The seven exclusive metabolic pathways corresponding to T2 were (1) glutathione metabolism, (2) pyruvate metabolism, (3) fatty acid degradation, (4) ketone body synthesis and degradation, (5) valine degradation, leucine and isoleucine, (6) propanoate metabolism,

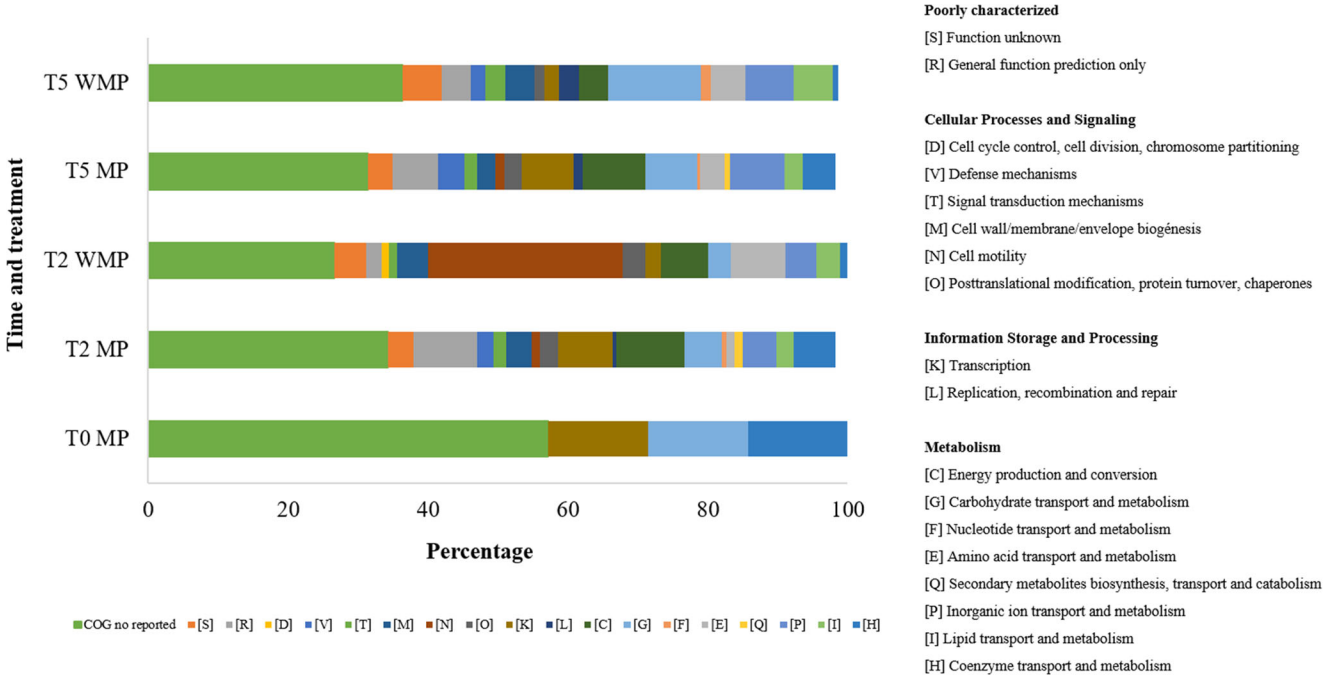

Fig. 4 Distribution of COG's in *B. cenocepacia* CEIB S5-2. T0, time 0 h; T2, time 2 h; T5, time 5 h

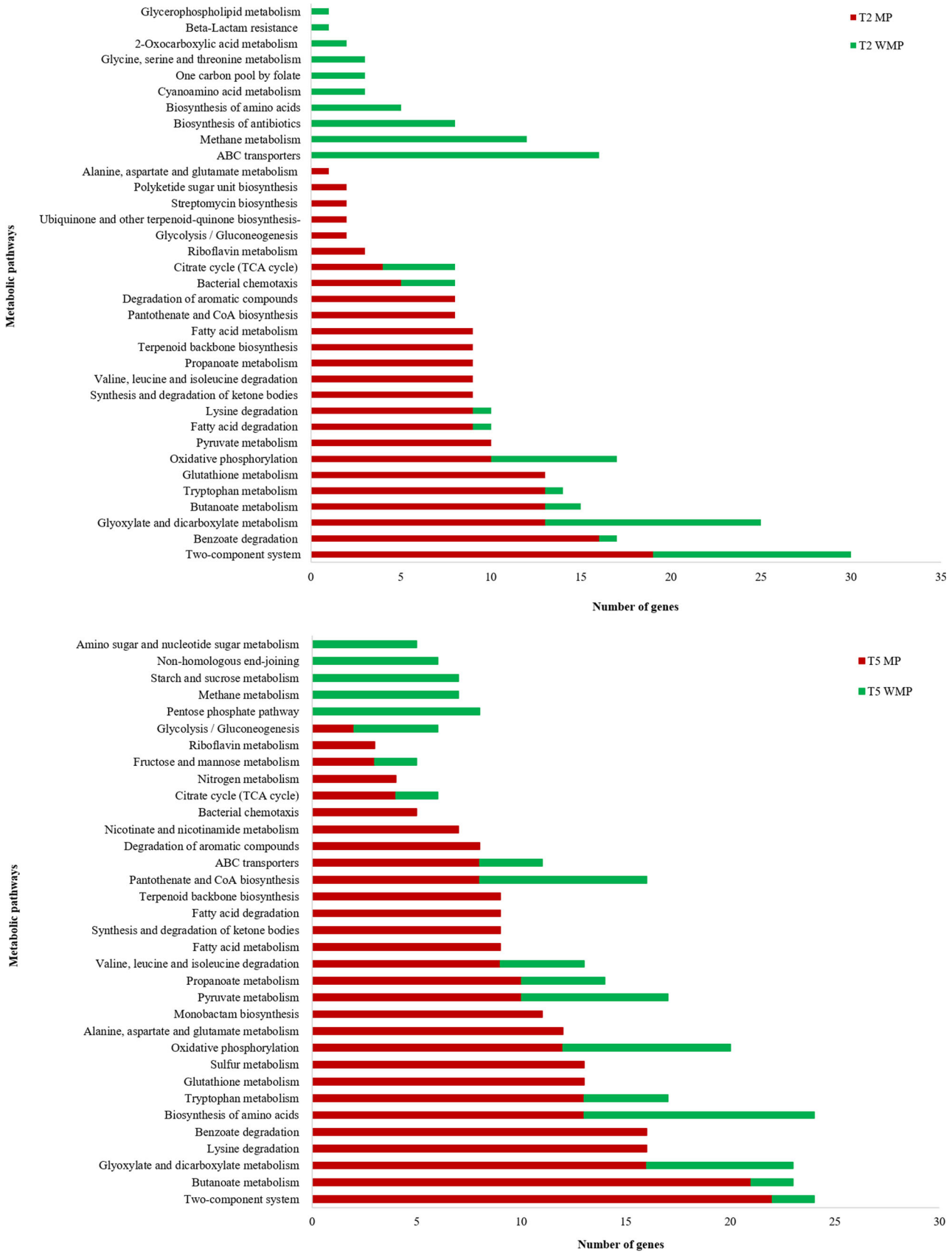

Fig. 5 Distribution of the DEGs of *B. cenocepacia* CEIB S5-2 in the KEGG maps at 2 h and five of incubation

and (7) degradation of aromatic compounds. The principal overrepresented metabolic pathways were the (1) two-component system, (2) benzoate degradation, (3) tryptophan metabolism, (4) glutathione metabolism, and (5) metabolism of butanoate. Finally, at the sampling time of 5 h, 107 of the 232 DEGs identified were located in metabolic pathways in KEEG; the exclusive metabolic pathways observed in T5 were (1) lysine degradation; (2) benzoate degradation; (3) glutathione metabolism; (4) sulfur metabolism; (5) alanine, aspartate metabolism, and glutamate; (6) biosynthesis of monobactam; (7) synthesis and degradation of ketone bodies; (8) degradation of fatty acids; and (9) metabolism of fatty acids. The overrepresented metabolic pathways in this condition were the following: (1) two-component system, (2) metabolism of butanoate, (3) metabolism of glyoxylate and dicarboxylate, (4) metabolism of tryptophan, and (5) metabolism of propanoate. For the control condition, the exclusive metabolic pathways observed were (1) carbon fixation in photosynthetic organisms, (2) pentose phosphate pathway, (3) methane metabolism, and (4) starch and sucrose metabolism (Fig. 5).

Transcriptional analysis of cluster *pnpABA'E1E2FDC*

According to the observed fold-change values, all genes that integrate the catabolic cluster *pnpABA'E1E2FDC* increased their expression levels in the presence of MP. This catabolic cluster includes the genes implicated in both PNP-degrading pathways. Regarding the expression levels of the HQ pathway genes, reported for PNP degradation in Gram-negative bacteria, at the beginning of the kinetics (T0), the genes *pnp*A (*p-nitrophenol monooxygenase*), *pnp*E1 (*hydroquinone 1,2-dioxygenase*, *subunit I*), and pnpE2 (*hydroquinone 1,2-dioxygenase*, *subunit II*) were the only genes of the catabolic cluster that showed differential expression with fold-change values of 1.8, 1.7, and 1.7 respectively. Subsequently, after 2 h of culture (T2), all the genes related with the PNP degradation through the HQ pathway presented a significant increase in their expression levels, showing the following fold-change values: *pnp*A, 9.3; *pnp*B (*p-benzoquinone reductase*), 9.1; *pnp*A′, 9.6; *pnp*E1, 9.1; *pnp*E2, 9.4; and *pnp*F (*4-hydroxymuconic semialdehyde dehydrogenase*), 8.7. After 5 h of culture (T5), all these genes reached their highest fold-change values: *pnp*A, 9.8; *pnp*B, 9.8; *pnp*A′, 9.6; *pnp*E1, 9.5; *pnp*E2, 9.9; and *pnp*F, 9.6 (Fig. 6).

On the other hand, after 2 h of culture (T2), the genes implicated in the BT pathway, reported for PNP degradation in Gram-positive bacteria, showed increases in their expression levels. The gene *pnp*C (*catechol 1,2-dioxygenase*), which catalyzes the breakdown of hydroxyquinol (BT) for obtaining maleylacetate, showed a fold-change value of 8.1. The gene of the ferredoxin dioxygenase subunit of the nitrate reductase, also known as ring-hydroxylating dioxygenase, showed a fold-change value of 7.8 in T2. The amino acid sequence encoded in this gene belongs to the Burkholderiaceae Rieske 2Fe-2S domain-containing proteins (Pfam PF00355). In bacteria, this group of redox proteins is implicated in the hydroxylation of different aromatic compounds (Haigler and Gibson, 1990; Martin and Mohn, 1999; Fishman et al., 2004). A gene with 97.7% similarity with the enzyme 4-nitrocatechol monooxygenase ferredoxin (Genebank: EKS70305.1) from *Burkholderia* sp. SJ98, a well-characterized strain capable of degrading nitroaromatic compounds, as PNP (Kumar et al., 2012), showed an increase in expression. 4-Nitrocatechol 4-monooxygenases are implicated in the catalytic hydroxylation of PNP to *p*-nitrocatechol and its subsequent transformation to 1,2,4 benzenetriol, the two initial enzymatic steps in the BT pathway. The gene of 4-nitrocatechol 4-monooxygenases is situated next to the sequence of the *pnp*C gene. Due to its proximity and enzymatic activity, this gene could be part of the PNP catabolic cluster in *B. cenocepacia* CEIB S5-2. After 5 h of culture (T5), both genes showed fold-change values of 9.0. Finally, both PNP-degrading metabolic pathways converge in the production of maleylacetate; the gene *pnp*D, which also is present in the catabolic cluster *pnpABA'E1E2FDC*, encodes for maleylacetate reductase, an enzyme that catalyzes the conversion of maleylacetate to β-ketoadipate. This gene also showed differential expression at T2 and T5, with respective fold-change values of 8.4 and 9.2. These findings indicate that *B. cenocepacia* CEIB S5-2 can overexpress all the genes of both PNP-degrading pathways (Fig. 6).

Relative expression of genes involved in MP hydrolysis and PNP degradation

The expression levels of the *mpd* gene, involved in the MP hydrolysis and the cluster *pnpABA'E1E2FDC*, which groups the genes related to PNP degradation, were evaluated through qRT-PCR. The relative expression of this set of genes in the experimental condition without MP was around 1.0 in all sampling times. However, as shown in Table 1, the *mpd* gene and the genes of the *pnpABA'E1E2FDC* cluster increased their expression levels over time. The genes *pnp*A′ and *pnp*E2 showed higher increases in relative expression levels ($2^{-\Delta\Delta C}{}_{T}$). In the sampling time of 5 h, the *pnp*A′ gene showed relative expression values over 10,000, while the relative expression values of the *pnp*E2 gene were around 7000. The overexpression of this set of genes observed in the qRT-PCR experiments is in concordance with the results of the differential expression analysis (fold-change) of the transcriptomic data.

Operon organization of the cluster *pnpABA'E1E2FDC*

The strain *B. cenocepacia* CEIB S5-2 presents all the genes that encode the enzymes related to the PNP degradation through the HQ (Gram-negative bacteria) and BT (Gram-positive bacteria) pathways. These genes are organized in a cluster

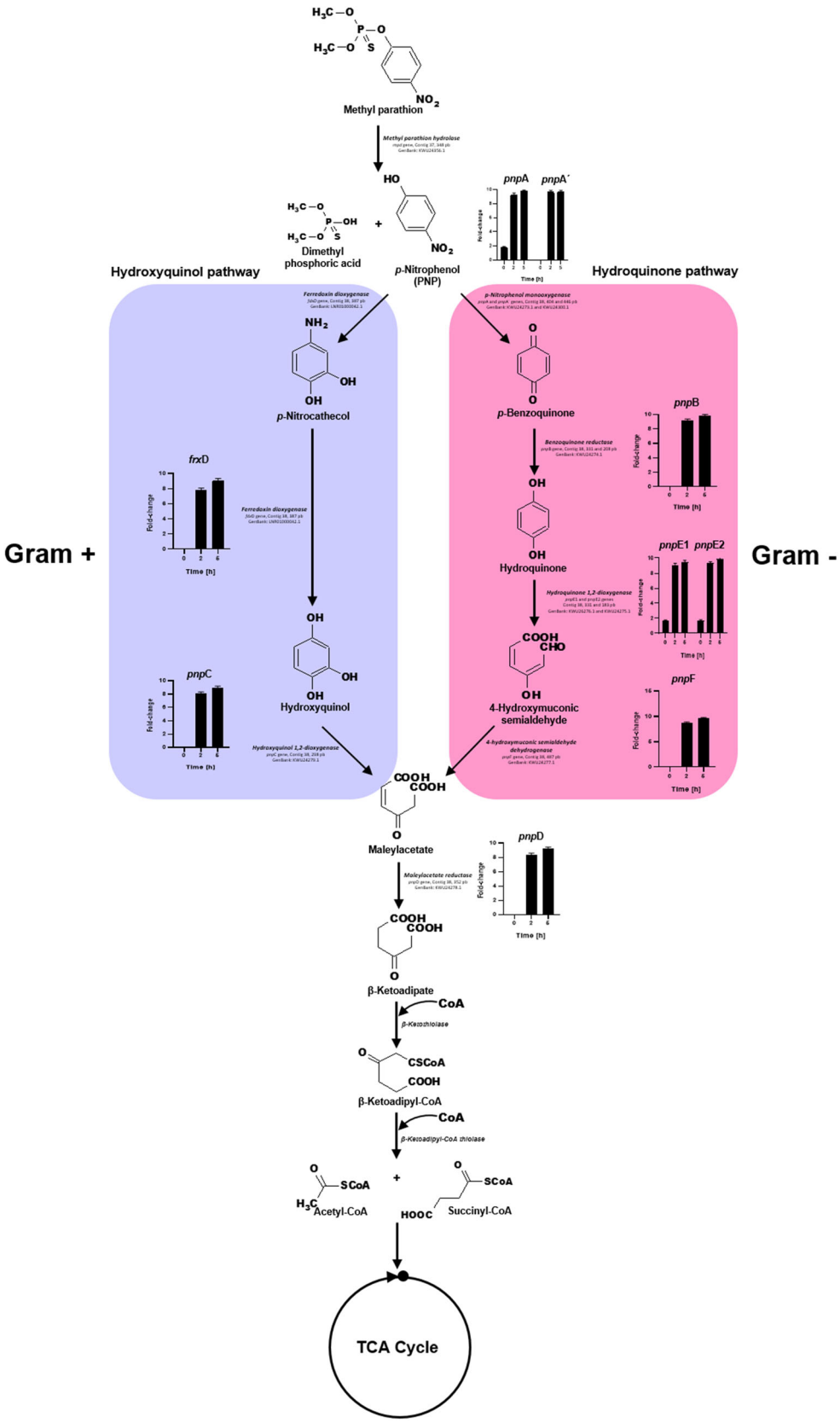

Fig. 6 Metabolic pathway used by *Burkholderia cenocepacia* CEIB S5-2 for MP hydrolysis and PNP degradation

pnpABA'E1E2FDC. As is shown in Fig. 7, all genes included in the cluster are translated in the same direction and show separations between genes lower than 470 bp. This distribution and direction of the genes included in the *pnpABA'E1E2FDC*

Table 1 Relative expression of *mpd* gene and *pnpABA'E1E2FDC* cluster. Average ± standard deviation and one-way analysis of variance to evaluate the effect to the sampling time (0, 2, and 5 h) on relative gene expression ($2^{-\Delta\Delta C}{}_T$)

Gene	Relative expression ($2^{-\Delta\Delta C}{}_T$)			
	T0	T2	T5	$F_{2,24}$
mpd	0.86 ± 0.03[a]	7.14 ± 0.19[b]	4.52 ± 0.42[c]	1322.48***
*pnp*A	5.98 ± 0.09[a]	781.44 ± 27.89[b]	1494.04 ± 155.70[c]	1024.65***
*pnp*B	2.89 ± 0.26[a]	935.76 ± 22.93[b]	3338.54 ± 301.24[c]	827.39***
*pnp*A´	3.03 ± 1.21[a]	9121.15 ± 170.24[b]	10,573.63 ± 2,760.74[b]	210.79***
*pnp*E1	5.19 ± 0.35[a]	1323.37 ± 32.43[b]	1337.20 ± 121.46[b]	1512.03***
*pnp*E2	33.71 ± 1.15[a]	458.25 ± 8.55[a]	7198.56 ± 1,663.00[b]	586.30***
*pnp*F	1.68 ± 0.39[a]	165.42 ± 16.90[b]	535.60 ± 54.05[c]	585.68***
*pnp*D	0.81 ± 0.06[a]	418.77 ± 20.22[b]	30.06 ± 2.71[c]	3216.05***
*pnp*C	0.84 ± 0.15[a]	424.61 ± 8.58[b]	888.36 ± 91.08[c]	546.76***
*fdx*D	0.98 ± 0.38[a]	290.02 ± 5.86[b]	900.76 ± 86.02[c]	1581.97***

T0, sampling time, 0 h; T2, sampling time, 2 h; T5, sampling time, 5 h

***$p < 0.0001$

The different letters denote statistically significant differences with a $p < 0.05$ (Tukey test).

cluster suggest that they could be organized in an operon. The results of the sequence analysis indicated the sequential organization of the genes of the PNP biodegradation pathway, with the presence of putative sites for translation promoters, situated in the − 10 and − 35 regions. The *pnpABA'E1E2FDC* cluster *pnpABA'E1E2FDC* from *B. cenocepacia* CEIB S5-2 was compared with similar gene cluster previously reported, as *Burkholderia* sp. SJ98 (Kumar et al., 2012), *B. zhejiangensis* CEIB S4-3 (Hernández-Mendoza et al. 2014), *Pseudomonas* sp. 1–7 (Zhang et al. 2012), *Pseudomonas* sp. WBC3 (Zhang et al., 2009a), *Pseudomonas* sp. NyZ402 (Wei et al. 2010), and *Pseudomonas putida* DLL-E4 (Shen et al., 2010). The analysis revealed the high sequence conservation of this gene cluster among species as *Burkholderia* sp. and *Pseudomonas* sp. (Fig. S2), displaying the higher similarity with the clusters from *Burkholderia* sp. SJ98 (*bit score* 8446) and *B. zhejiangensis* CEIB S4-3 (*bit score* 8278). To evaluate the operon organization of the gene cluster *pnpABA'E1E2FDC*, different sequential and overlapping segments were PCR amplified using the following oligonucleotide pairs *pnpAf-pnpBr*, *pnpE1f-pnpFr*, *pnpFf-pnpDr*, and *pnpCf-fdxDr*; in Table S1, the sequence of the oligonucleotide employed and the expected amplicon size are shown; the PCR amplification products showed molecular weights in the range of the theoretical expected values for each oligonucleotide pairs (Fig. S3). Additionally, the co-expression of the evaluated genes was verified, indicating the operon conformation of the genetic cluster.

Discussion

According to the genomic data, *B. cenocepacia* CEIB S5-2 presents all the genes implicated in the biodegradation of PNP through the HQ pathway, which is a characteristic of Gram-negative bacteria. This strain also presents genes implicated in the PNP biodegradation through the BT pathway, mainly

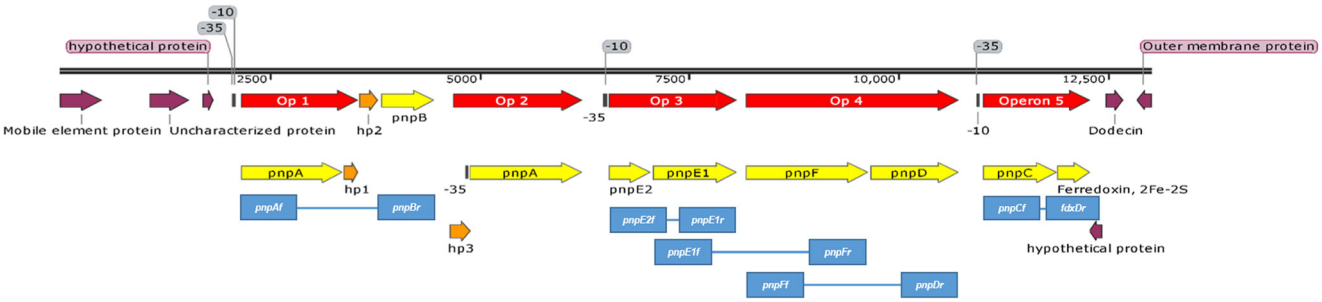

Fig. 7 Operon conformation of the *pnpABA'E1E2FDC* gene cluster. The genome location of the PNP-degrading genes is shown; arrows indicate the direction of the translation. Op, predicted operons; hp, genes encoding hypothetical proteins; *−10* and *−35*, transcription promoter regions; *pnp*A, gene encoding *p-nitrophenol-4-monoxygenase*; *pnp*B, gene encoding *p-benzoquinone reductase*; *pnp*E2/E1, gene encoding *hydroquinone-1,2-dioxygenase*; *pnp*F, gene encoding *4-hdroxymuconic semialdehyde dehydrogenase*; *pnp*D, gene coding for *maleylacetate reductase*; *pnp*C, gene encoding *1,2,4-benzenetriol dioxygenase*; and *fdxD*, gene coding for ferredoxin dioxygenase subunit of the nitrate reductase. The image was built in SnapGene viewer (SnapGene software, Insightful Science, San Diego, CA, USA)

characterized in Gram-positive bacteria. Previous works have described the presence of both PNP-degrading pathways in Gram-negative bacteria as *Burkholderia* sp. SJ98 (Vikram et al., 2013), *Burkholderia zhejiangensis* CEIB S4-3 (Castrejón-Godínez et al., 2019), and *Pseudomonas* sp. strain WBC-3 (Zhang et al., 2009b). However, it is important to highlight that *B. cenocepacia* CEIB S5-2 can biodegrade PNP in only 5 h, while *Burkholderia* sp. SJ98 can biodegrade PNP in soil (45 mg/Kg) in 16 days (Min et al., 2017), and *Burkholderia zhejiangensis* CEIB S4-3 can biodegrade PNP in solution (50 mg/L) in 12 h.

The first step in the BT pathway is the conversion of PNP to *p*-nitrocatechol; subsequently this metabolite is converted to 1,2,4-benzenetriol in the second step of the pathway; these reactions are catalyzed by the enzyme *p*-nitrophenol monooxygenase-II, in Gram-positive bacteria as *Arthrobacter* sp. (Jain et al., 1994), *Bacillus sphaericus* JS905 (Kadiyala et al., 1998), and *Rhodococcus opacus* SAO101 (Kitagawa et al., 2004). However, the gene which encodes for *p*-nitrophenol monooxygenase-II has not been identified in the *B. cenocepacia* CEIB S5-2 genome. The presence of all genes implicated in the HQ pathway and the presence of the *pnp*C gene from the BT pathway suggest that the strain could degrade PNP and other aromatic compounds through both metabolic pathways. Vikram et al. (2012) studied the PNP degradation pathway present in *Burkholderia* sp. SJ98, a bacterial strain that can use PNP as the sole carbon source. In the study, all genes of the HQ degradation pathway were identified. However, as in the present work, just the gene *pnp*C of the BT pathway was identified; the authors could not establish if *Burkholderia* sp. SJ98 can use the BT pathway simultaneously with the HQ pathway for PNP degradation. The genomic data of *Burkholderia* sp. SJ98 revealed the presence of the gene EKS70305.1 which encodes for a 4-nitrocatechol monooxygenase ferredoxin protein; this enzyme can catalyze the two initial enzymatic steps in the BT pathway; in *B. cenocepacia* CEIB S5-2 was identified a gene with 97.7% sequence similarity with the enzyme 4-nitrocatechol monooxygenase ferredoxin from *Burkholderia* sp. SJ98.

The genomic conformation and sequences of the catalytic gene clusters implicated in the PNP biodegradation are highly conserved in bacterial strains isolated from PNP-contaminated sites. The catalytic cluster *pnpABA'E1E2FDC* of *B. cenocepacia* CEIB S5-2 shows great similarity with the PNP catabolic clusters identified in *Burkholderia* sp. SJ98 (Vikram et al., 2012) and *B. zhejiangensis* CEIB S4-3 (Castrejón-Godínez et al., 2019). The strain *B. zhejiangensis* CEIB S4-3 was isolated from agricultural soils from Tepoztlán, in the state of Morelos, Mexico, at the same sampling location as *B. cenocepacia* CEIB S5-2. The high sequence similarity between the PNP catabolic clusters of both strains suggest events of horizontal transference of the PNP-degrading genes between the strains. In *Burkholderia* sp. SJ98, the genes *pnp*E1 and *pnp*E2 encoded for an Fe(II)-dependent heterodimeric protein that catalyzes the hydroquinone transformation to 4-hydroxymuconic semialdehyde, the genes *pnp*E1 and *pnp*E2 from *B. cenocepacia* CEIB S5-2 show great sequence similarity with the genes from *Burkholderia* sp. SJ98, suggesting the formation of E1/E2 heterodimers.

According to the results of the DEGs and PCA analyses, the presence of MP in the culture media induces the expression of genes that encode transcriptional regulators in the *B. cenocepacia* CEIB S5-2 strain; 9 and 13 DEGs with this function were identified at the sampling times of 2 and 5 h, respectively; these genes corresponded to the 1 and 2% of the total DEGs identified at such sampling times. These findings suggest that the MP hydrolysis and the PNP degradation require complex transcriptional regulation. As was previously reported by Chakka et al. (2015), Chen et al. (2016), and Castrejón-Godínez et al. (2019), the transcriptional regulation is not limited to the genes involved in the PNP degradation but also require the regulation of transcriptional and metabolic processes.

The exposure to MP induces the overexpression of genes from different metabolic pathways. The transcriptional profile of *B. cenocepacia* CEIB S5-2 in the presence of MP shows an overexpression in genes from the TCA pathway at 5 h; in prior sampling times, these genes did not show differences in the expression with respect to the control condition. Similar findings were observed with glyoxylate metabolism. In limited carbon source conditions, the glyoxylate cycle plays an important role in the carbohydrate synthesis from oxalacetate, a molecule generated by the joining of two acetyl-CoA molecules derived from fatty acid reserve degradation. The PNP degradation generates two intermediate metabolites of the TCA pathway, acetyl-CoA and succinyl-CoA. In the presence of MP, after 2 and 5 post-inoculation hours, different genes related to the degradation of the aromatic compounds showed a significant overexpression. In the study of Chen et al. (2016), the transcriptional profile of *P. putida* DLL-E4 in the presence of PNP and glucose as carbon sources revealed the overexpression of key enzymes from the TCA cycle, in contrast to the control condition in the presence of glucose as the sole carbon source. On the other side, Lu et al. (2013) evaluated the adverse effects related to the organophosphorus herbicide glyphosate exposure in *E. coli*; the transcriptional analysis revealed that the inhibition of essential enzymes from the pentose phosphate pathway, TCA cycle, and gluconeogenesis caused an inhibition of bacterial growth. The overexpression of genes from the TCA cycle seems to play a key role in the PNP degradation capabilities in bacteria.

At the beginning of the kinetics in the presence of MP, the transcriptional analysis shows the overexpression of a gene that encodes the dominium-denominated GAF from a histidine kinase, a key protein in the two-component signal transduction

system. These signal transduction systems are predominant in sensing environmental changes and coupling the cellular physiological responses in bacteria (Capra and Laub, 2012). In the report of Lau et al. (1997), the exposure of *P. putida* F1 to the aromatic hydrocarbon toluene induced the overexpression of the genes *todS* and *todT*. These genes encode for a histidine kinase sensor and its transcriptional regulator, respectively, integrating a two-component signal transduction system. In recent work, it was reported that the expression of the *tod* operon is related to the regulation of the toluene degradation pathway in *P. putida* (Koh et al., 2016). Also, through proteome and qRT-PCR analyses, Tiwari et al. (2018) proposed that a two-component signal transduction system triggers the induction of proteins related to oxidative stress contention and biodegradation MP in *Fischerella* sp. Another early overexpressed gene by *B. cenocepacia* CEIB S5-2 in the presence of MP was a translational regulator of the family *TetR*, commonly overexpressed in bacterial strains as a response to the stress caused by the use of alternative carbon sources in the cultures. The *TetR* transcriptional regulators are also implicated in the environmental stimuli response, multidrug-resistance, *quorum-sensing*, osmotic stress, and biofilm formation (Cuthbertson and Nodwell, 2013; Le Minh et al., 2015; Colclough et al., 2019). In cultures of *Fischerella* sp., the presence of MP induced the overexpression of the *TetR* gene (Tiwari et al., 2018). According to these findings, it could be possible that the *TetR* gene plays a key role in the MP recognizing, activation of the PNP catabolic cluster, and modulation of the physiological stress response in *B. cenocepacia* CEIB S5-2.

The participation of different transcriptional regulators has been reported for the degradation of PNP and its derived metabolites. Takeo et al. (2008) reported an *AraC* type (*NphR*) transcriptional regulator implicated in the PNP oxidation in *Rhodococcus* sp. PN1. Shen et al. (2010) identified a *LysR*-type transcriptional regulator implicated in the hydroquinone degradation in *P. putida* DLL-E4; the mutation-mediated elimination of the LTTR gene caused the loss of the ability for degrading hydroquinone in the strain. Zhang et al. (2009b) described the importance of the *pnpR* gene, a *LysR*-type transcriptional regulator, to activate the expression of the operon that mediates the PNP degradation in *Pseudomonas* sp. WBC-3. In the present study, at the sampling time of 5 h in the presence of MP, *B. cenocepacia* CEIB S5-2 showed the overexpression of genes that encode for *AraC*- and *LysR*-type transcriptional regulators. Genes that encode for other types of transcriptional regulators as *LuxR*, reported as a *quorum-sensing* regulator (Chen and Xie, 2011); *GntR*, implicated in the regulation of biofilm formation and multiple sugar transport (Li et al., 2019); and *ArsR*, implicated in metal sensing in different bacteria (Osman and Cavet 2010), also showed an overexpression in the presence of MP; however, the role of these genes in pesticide degradation is still unknown.

The presence of MP in the culture caused the early (T0) overexpression of two genes that encode for a permease and a cellular transporter, both belonging to the mayor facilitator superfamily (MFS) (InterPro: IPR036259). According to the BLAST analysis, the amino acid sequences of such genes showed high similarity, above 90%, with transporters of the MFS family in *Burkholderia* sp. SJ98 and *Burkholderia* sp. YI23, respectively. These bacterial strains were isolated from contaminated environments and are capable of degrading the organophosphate insecticide fenitrothion and PNP; the expression of these cellular transporters could play an essential role for the uptake of these xenobiotics during the degradation process in these bacterial strains (Lim et al., 2012; Kumar et al., 2012). In the transcriptomic study of *B. zhejiangensis*, CEIB S4-3 in the presence of MP observed the overexpression of genes that encode for different transporters such as *GntR*, *AraC*, and *MerR* (Castrejón-Godínez et al., 2019). Transporters are membrane proteins essential for nutrient uptake and the exporting of metabolites and toxic substances from the cell. The MFS transporter family are of the most preponderant proteins in the transport of drugs, ions, sugar, sugar phosphates, and hydrophobic compounds (Jiang et al., 2013; Zomot et al., 2018; Huang et al., 2003). The overexpression of cellular transporters in the presence of MP in *B. cenocepacia* CEIB S5-2 could be implicated in the pesticide uptake at the beginning of the culture.

After 2 incubation hours in the presence of MP, the highest PNP concentration in the culture was observed. At this time, the overexpression of a gene that encodes for a protein of the universal stress protein family (*Usp*) was observed; these are cytoplasmic proteins whose expression is altered as a consequence of different internal or external stress conditions (Kvint et al., 2003; Vollmer and Bark, 2018). The Usp-proteins are essential to overcome oxidative stress in *E. coli*. The absence of the UspA gene in a mutant strain caused premature cellular death, while its exacerbated expression causes and bacterial growth arrest (Nachin et al., 2005). Exposure to pesticides causes diverse stressor conditions over microorganisms (Stanley and Preetha 2016). At the same sampling time (T2), it was observed the overexpression of a gene that encodes for an RNA polymerase sigma-70 factor. The sigma factor family members have the function of directing the general transcription in bacteria, serving as contact points for regulatory proteins, and are also expressed in response to stressing conditions that menace the cell wall and the membrane integrity (Paget and Helmann, 2003). The overexpression of the *Usp* and the RNA polymerase sigma-70 factor genes at the time of 2 h indicates that the high concentration of PNP induces cellular stress in *B. cenocepacia* CEIB S5-2; the bacterial capability to tolerate or overcome the adverse effects of exposure to pesticides is a vital characteristic in bacterial strains with high pesticide degradation profiles.

At the sampling times 2 and 5 h, the overexpression of different genes that encode for efflux proteins were observed. As the gene that encodes for a subunit of the outer membrane

protein (*oprM*), the gene that encodes for the permease subunit of a resistance-nodulation-division (RND)-type efflux pump, and the gene that encode for the adapter subunit of an RND-type efflux pump. The efflux systems are key proteins for the resistance to different toxic chemical compounds, mostly in multidrug-resistant bacteria, because these systems actively expulse these toxic compounds to the extracellular media (Akama et al., 2004; Symmons et al., 2009; Phan et al., 2010; Blanco et al., 2016). Moreover, it has been reported that efflux pumps are also important in the tolerance and resistance to pesticides (Nikaido et al., 2011) and oxidative stress contention (Bogomolnaya et al., 2013).

At the sampling time of 5 h, different genes that encode for proteins implicated in the oxidative stress damage contention were overexpressed. Two genes that encode for the C and D subunits of the enzyme alkyl-hydroperoxide reductase (*Ahp*) were observed. This kind of proteins protect the cell from oxidative stress by reducing the hydrogen peroxide (Bryk et al., 2002; Nunn et al., 2002). In *Fischerella* sp., it has been reported that the exposition to MP causes the release of reactive oxygen species after 2 and 8 exposure days (Tiwari et al., 2018). Chen et al. (2016) observed the overexpression of genes related to the contention of oxidative stress in *P. putida* DLL-E4 exposed to PNP.

In the transcriptomic analysis with MP, different genes implicated in the PNP degradation were identified. As a gene that showed a 100% amino acid sequence identity and coverture with the enzyme *p*-nitrophenol monooxygenase from the *Burkholderiaceae* family (*pnpA* gene), an FDA-dependent monooxygenase catalyzes the hydroxylation of PNP to generate *p*-benzoquinone and release of nitrate. In the genes that encode the sequences of the large subunit of the same enzyme hydroquinone 1,2 dioxygenase (*pnpE1*) and the small subunit of the same enzyme (*pnpE2*), both sequences showed high amino acid sequence similitude, 82.2 and 99.4%, respectively, with *pnp*E1 and *pnp*E2 from *Burkholderia* sp. SJ98. Hydroquinone 1,2 dioxygenase catalyzes the aromatic ring opening of hydroquinone to produce 4-hydroxy muconic semialdehyde in the hydroquinone pathway for PNP degradation (Liu et al., 2015; Chen et al., 2016). In the transcriptomic analysis, all genes implicated in the PNP degradation showed differential expression across the kinetics supplemented with MP; in a similar way all genes of the *pnpABA'E1E2FDC* cluster showed a significant overexpression in the qRT-PCR experiments.

Besides, genes from several metabolic pathways show differential expression in the presence of MP, such as oxidative phosphorylation, sulfur metabolism, amino acids biosynthesis, and the TCA cycle; the overexpression of these metabolic pathways suggests that the strain can use MP and PNP as carbon source and for energy generation, necessary for the maintenance of the bacterial population and the slightly bacterial growth observed during the kinetics. Similar findings were observed with the bacterial strain *B. zhejiangensis* CEIB S4-3 (Castrejón-Godínez et al., 2019).

Conclusions

B. cenocepacia CEIB S5-2 is a strain with the capability of hydrolyze MP and degrade PNP in 5 h. This capability is related with the expression of hydrolytic enzymes encoded in the *mpd* gene and the PNP degradation cluster *pnpABA'E1E2FDC* organized as an operon.

Regarding the transcriptome analysis, in general, the observed expression changes in *B. cenocepacia* CEIB S5-2 genes are related to the ability to fight with the stress caused by the presence of MP in the media. The observed overexpression of transporters, permeases, and porins in the MP condition suggests an increase in the transport and exchange of molecules with the surrounding media; the overexpression of these kind of proteins could be an essential mechanism to lie with the toxicity caused by the presence of MP, PNP, and the metabolites derived from the PNP degradation. The observed capability of the strain for degrading PNP in the range of 5 h could be related to the presence of genes from both HQ and BT PNP degradation pathways, a significant overexpression in all the genes of the *pnpABA'E1E2FDC* cluster, as was observed in both transcriptome and qRT-PCR experiments, thus increasing the efficiency of the biodegradation process.

At the end of the kinetics, 5 h, the transcriptional analysis revealed the overexpression of exclusive genes related to the oxidative stress response, probably as a defense mechanism towards the toxic effects caused by PNP. On the other hand, the overexpression of genes related with aromatic compounds and amino acid metabolism, as well as oxidative phosphorylation, suggests that the strain could use the pesticide as a carbon and energy source and for the maintenance of the bacterial population. *B. cenocepacia* CEIB S5-2 has a great potential for its application in pesticide bioremediation approaches due to its high PNP biodegradation capability and the expression of resistance mechanisms to avoid the stress generated by the PNP exposure. In future studies, the genes related to the PNP biodegradation could be cloned in suitable organisms, and the enzymes can be produced by the use of a heterologous expression system for their subsequent application in pesticide bioremediation strategies.

Supplementary Information The online version contains supplementary material available at https://doi.org/10.1007/s11356-021-13647-6.

Acknowledgements This work was supported by for the National Council for Science and Technology (CONACyT for its acronym in

Spanish). The funders had no role in study design, data collection and analysis, decision to publish, or preparation of the manuscript.

Author contribution Ma. Laura Ortiz-Hernández, Alexis Rodríguez, and Patricia Mussali-Galante conceived and designed the experiments; contributed with reagents, materials, and analysis tools; and conducted data analysis and the manuscript writing. Yitzel Gama-Martínez, Maikel Fernández-López, and Emmanuel Salazar conducted experiments. María Luisa Castrejón-Godínez prepared the figures and tables and redacted the manuscript. Sergio Encarnación and Efraín Tovar-Sánchez analyzed the data and contributed with reagents, materials, and analysis tools. All authors read and approved the manuscript.

Funding information The present study was founded by the National Council for Science and Technology (CONACyT), grant No. CB2014-240414.

Availability of the data Genomic data are available at NCBI with the following BioProject accession PRJNA 301637.

Declarations

Ethics approval The present study does not contain any studies with humans or animals performed by any of the authors.

Consent to participate and consent for publication All authors and institutions where the work was carried out have approved the content and authorship of the manuscript.

Conflict of interest The authors declare that they have no conflict of interest.

References

Akama H, Kanemaki M, Yoshimura M, Tsukihara T, Kashiwagi T, Yoneyama H, Narita SI, Nakegawa A, Nakae T (2004) Crystal structure of the drug discharge outer membrane protein, OprM, of Pseudomonas aeruginosa dual modes of membrane anchoring and occluded cavity end. J Biol Chem 279(51):52816–52819. https://doi.org/10.1074/jbc.C400445200

Bhatt P, Zhou X, Huang Y, Zhang W, Chen S (2021) Characterization of the role of esterases in the biodegradation of organophosphate, carbamate, and pyrethroid pesticides. J Hazard Mater 411(5):125026

Blanco P, Hernando-Amado S, Reales-Calderon JA, Corona F, Lira F, Alcalde-Rico M, Bernardini A, Sanchez MB, Martinez JL (2016) Bacterial multidrug efflux pumps: much more than antibiotic resistance determinants. Microorganisms 4(1):14. https://doi.org/10.3390/microorganisms4010014

Bogomolnaya LM, Andrews KD, Talamantes M, Maple A, Ragoza Y, Vazquez-Torres A, Andrews-Polymenis H (2013) The ABC-type efflux pump MacAB protects Salmonella enterica serovar typhimurium from oxidative stress. MBio 4(6):e00630–e00613. https://doi.org/10.1128/mBio.00630-13

Bryk R, Lima CD, Erdjument-Bromage H, Tempst P, Nathan C (2002) Metabolic enzymes of mycobacteria linked to antioxidant defense by a thioredoxin-like protein. Science 295(5557):1073–1077. https://doi.org/10.1126/science.1067798

Capra EJ, Laub MT (2012) Evolution of two-component signal transduction systems. Annu Rev Microbiol 66:325–347. https://doi.org/10.1146/annurev-micro-092611-150039

Castrejón-Godínez ML, Ortiz-Hernández ML, Salazar E, Encarnación S, Mussali-Galante P, Tovar-Sánchez E, Sánchez-Salinas E, Rodríguez A (2019) Transcriptional analysis reveals the metabolic state of Burkholderia zhejiangensis CEIB S4-3 during methyl parathion degradation. PeerJ 7:e6822. https://doi.org/10.7717/peerj.6822

Chakka D, Gudla R, Madikonda AK, Pandeeti EVP, Parthasarathy S, Nandavaram A, Siddavattam D (2015) The organophosphate degradation (opd) Island-borne esterase induced metabolic diversion in Escherichia coli and its influence on p-Nitrophenol degradation. J Biol Chem 290(50):29920–29930. https://doi.org/10.1074/jbc.M115.661249

Chen J, Xie J (2011) Role and regulation of bacterial LuxR-like regulators. J Cell Biochem 112(10):2694–2702. https://doi.org/10.1002/jcb.23219

Chen Q, Tu H, Luo X, Zhang B, Huang F, Li Z, Wang J, Shen W, Wu J, Cui Z (2016) The regulation of para-nitrophenol degradation in Pseudomonas putida DLL-E4. PLoS One 11(5):e0155485. https://doi.org/10.1371/journal.pone.0155485

Colclough AL, Scadden J, Blair JMA (2019) TetR-family transcription factors in Gram-negative bacteria: conservation, variation and implications for efflux-mediated antimicrobial resistance. BMC Genomics 20(1):731. https://doi.org/10.1186/s12864-019-6075-5

Cuthbertson L, Nodwell JR (2013) The TetR family of regulators. Microbiol Mol Biol Rev 77(3):440–475. https://doi.org/10.1128/MMBR.00018-13

Dorneles AL, de Souza RA, Blochtein B (2017) Toxicity of organophosphorus pesticides to the stingless bees *Scaptotrigona bipunctata* and Tetragonisca fiebrigi. Apidologie 48(5):612–620. https://doi.org/10.1007/s13592-017-0502-x

Fernández-López MG, Popoca-Ursino C, Sánchez-Salinas E, Tinoco-Valencia R, Folch-Mallol JL, Dantán-González E, Ortiz-Hernández ML (2017) Enhancing methyl parathion degradation by the immobilization of *Burkholderia* sp. isolated from agricultural soils. MicrobiologyOpen 6:e507. https://doi.org/10.1002/mbo3.507

Fishman A, Tao Y, Bentley WE, Wood TK (2004) Protein engineering of toluene 4-monooxygenase of Pseudomonas mendocina KR1 for synthesizing 4-nitrocatechol from nitrobenzene. Biotechnol Bioeng 87(6):779–790. https://doi.org/10.1002/bit.20185

Fosu-Mensah BY, Okoffo ED, Darko G, Gordon C (2016) Organophosphorus pesticide residues in soils and drinking water sources from cocoa producing areas in Ghana. Environ Syst Res 5(1):1–12. https://doi.org/10.1186/s40068-016-0063-4

Galperin MY, Makarova KS, Wolf YI, Koonin EV (2014) Expanded microbial genome coverage and improved protein family annotation in the COG database. Nucleic Acids Res 43(D1):D261–D269. https://doi.org/10.1093/nar/gku1223

Haigler BE, Gibson DT (1990) Purification and properties of NADH-ferredoxinNAP reductase, a component of naphthalene dioxygenase from Pseudomonas sp. strain NCIB 9816. J Bacteriol 172(1):457–464. https://doi.org/10.1128/jb.172.1.457-464.1990

Hammer Ø, Harper DA, Ryan PD (2001) PAST: Paleontological statistics software package for education and data analysis. Palaeontol Electron 4(1):1–9

Hernández-Mendoza A, Martínez-Ocampo F, Lozano-Aguirre Beltrán LF, Popoca-Ursino EC, Ortiz-Hernández L, Sánchez-Salinas E, Dantán-González E (2014) Draft genome sequence of the organophosphorus compound-degrading Burkholderia zhejiangensis strain CEIB S4-3. Genome Announc 2(6):e01323–14. https://doi.org/10.1128/genomeA.01323-14

Horne I, Sutherland TD, Oakeshott JG, Russell RJ (2002) Cloning and expression of the phosphotriesterase gene hocA from Pseudomonas monteilii C11bbThe GenBank accession number for the hocA gene is AF469117. Microbiology 148(9):2687–2695. https://doi.org/10.1099/00221287-148-9-2687

Huang Y, Lemieux MJ, Song J, Auer M, Wang DN (2003) Structure and mechanism of the glycerol-3-phosphate transporter from

Escherichia coli. Science. 301(5633):616–620. https://doi.org/10.1126/science.1087619

Jain RK, Dreisbach JH, Spain JC (1994) Biodegradation of p-nitrophenol via 1, 2, 4-benzenetriol by an Arthrobacter sp. Appl Environ Microbiol 60(8):3030–3032

Jiang D, Zhao Y, Wang X, Fan J, Heng J, Liu X, Feng W, Kang X, Huang B, Liu J, Zhang XC (2013) Structure of the YajR transporter suggests a transport mechanism based on the conserved motif A. Proc Natl Acad Sci 110(36):14664–14669. https://doi.org/10.1073/pnas.1308127110

Jokanović M (2018) Neurotoxic effects of organophosphorus pesticides and possible association with neurodegenerative diseases in man: a review. Toxicology 410:125–131. https://doi.org/10.1016/j.tox.2018.09.009

Kadiyala V, Smets BF, Chandran K, Spain JC (1998) High affinity p-nitrophenol oxidation by Bacillus sphaericus JS905. FEMS Microbiol Lett 166(1):115–120. https://doi.org/10.1111/j.1574-6968.1998.tb13191.x

Karasali H, Maragou N (2016) Pesticides and herbicides: types of pesticide. Encycl Food Health:319–325. https://doi.org/10.1016/B978-0-12-384947-2.00535-3

Kitagawa W, Kimura N, Kamagata Y (2004) A novel p-nitrophenol degradation gene cluster from a gram-positive bacterium, *Rhodococcus opacus* SAO101. J Bacteriol 186(15):4894–4902. https://doi.org/10.1128/JB.186.15.4894-4902.2004

Koh S, Hwang J, Guchhait K, Lee EG, Kim SY, Kim S, Lee S, Chung JM, Jung HS, Lee SJ, Ryu CM, Lee SG, Oh TK, Kwon O, Kim MH (2016) Molecular insights into toluene sensing in the TodS/TodT signal transduction system. J Biol Chem 291(16):8575–8590. https://doi.org/10.1074/jbc.M116.718841

Kulkarni M, Chaudhari A (2006) Biodegradation of p-nitrophenol by P. putida. Bioresour Technol 97(8):982–988. https://doi.org/10.1016/j.biortech.2005.04.036

Kumar S, Vikram S, Raghava GPS (2012) Genome sequence of the nitroaromatic compound-degrading bacterium Burkholderia sp. strain SJ98. Genome Announc 194(12):3286. https://doi.org/10.1128/JB.00497-12

Kvint K, Nachin L, Diez A, Nyström T (2003) The bacterial universal stress protein: function and regulation. Curr Opin Microbiol 6(2):140–145. https://doi.org/10.1016/S1369-5274(03)00025-0

Lau PC, Wang Y, Patel A, Labbé D, Bergeron H, Brousseau R, Konishi Y, Rawlings M (1997) A bacterial basic region leucine zipper histidine kinase regulating toluene degradation. Proc Natl Acad Sci 94(4):1453–1458. https://doi.org/10.1073/pnas.94.4.1453

Le Minh PN, de Cima S, Bervoets I, Maes D, Rubio V, Charlier D (2015) Ligand binding specificity of RutR, a member of the TetR family of transcription regulators in Escherichia coli. FEBS Open Biol 5:76–84. https://doi.org/10.1016/j.fob.2015.01.002

Li Z, Xiang Z, Zeng J, Li Y, Li J (2019) A GntR family transcription factor in Streptococcus mutans regulates biofilm formation and expression of multiple sugar transporter genes. Front Microbiol 9:3224. https://doi.org/10.3389/fmicb.2018.03224

Lim JS, Choi BS, Choi AY, Kim KD, Kim DI, Choi IY, Ka JO (2012) Complete genome sequence of the fenitrothion-degrading *Burkholderia* sp. strain YI23. J Bacteriol 194:896–811. https://doi.org/10.1128/JB.06479-11

Liu S, Su T, Zhang C, Zhang WM, Zhu D, Su J, Zhou NY, Xu S (2015) Crystal structure of PnpCD, a two-subunit hydroquinone 1, 2-dioxygenase, reveals a novel structural class of Fe2+-dependent dioxygenases. J Biol Chem 290(40):24547–24560. https://doi.org/10.1074/jbc.M115.673558

Livak KJ, Schmittgen TD (2001) Analysis of relative gene expression data using real-time quantitative PCR and the $2^{-\Delta\Delta CT}$ method. Methods 25(4):402–408. https://doi.org/10.1006/meth.2001.1262

Love MI, Huber W, Anders S (2014) Moderated estimation of fold change and dispersion for RNA-seq data with DESeq2. Genome Biol 15(12):550. https://doi.org/10.1186/s13059-014-0550-8

Lu W, Li L, Chen M, Zhou Z, Zhang W, Ping S, Yan Y, Wang J, Lin M (2013) Genome-wide transcriptional responses of Escherichia coli to glyphosate, a potent inhibitor of the shikimate pathway enzyme 5-enolpyruvylshikimate-3-phosphate synthase. Mol BioSyst 9(3):522–530. https://doi.org/10.1039/C2MB25374G

Martin M (2011) Cutadapt removes adapter sequences from high-throughput sequencing reads. EMBnet J 17(1):10–12. https://doi.org/10.14806/ej.17.1.200

Martin VJ, Mohn WW (1999) A novel aromatic-ring-hydroxylating dioxygenase from the diterpenoid-degrading bacterium Pseudomonas abietaniphila BKME-9. J Bacteriol 181(9):2675–2682. https://doi.org/10.1128/JB.181.9.2675-2682.1999

Martínez-Ocampo F, López MGF, Beltrán LFLA, Popoca-Ursino EC, Ortiz-Hernández ML, Sánchez-Salinas E, Ramos-Quintana F, Villalobos-López MA, Dantán-González E (2016) Draft genome sequence of *Burkholderia cenocepacia* strain CEIB S5-2, a methyl parathion-and p-Nitrophenol-degrading bacterium, isolated from agricultural soils in Morelos, Mexico. Genome Announc 4(2):e00220–e00216. https://doi.org/10.1128/genomeA.00220-16

Megharaj M, Pearson HW, Venkateswarlu K (1991) Toxicity of p-aminophenol and p-nitrophenol to Chlorella vulgaris and two species of Nostoc isolated from soil. Pestic Biochem Physiol 40(3):266–273. https://doi.org/10.1016/0048-3575(91)90098-7

Min J, Wang B, Hu X (2017) Effect of inoculation of Burkholderia sp. strain SJ98 on bacterial community dynamics and para-nitrophenol, 3-methyl-4-nitrophenol, and 2-chloro-4-nitrophenol degradation in soil. Sci Rep 7(1):1–9. https://doi.org/10.1038/s41598-017-06436-0

Mulbry WW, Karns JS (1989) Parathion hydrolase specified by the Flavobacterium opd gene: relationship between the gene and protein. J Bacteriol 171(12):6740–6746. https://doi.org/10.1128/jb.171.12.6740-6746.1989

Mulla SI, Ameen F, Talwar MP, Eqani SAMAS, Bharagava RN, Saxena G, Tallur PN, Ninnekar HZ (2020) Organophosphate pesticides: impact on environment, toxicity, and their degradation. In: Saxena G, Bharagava RN (eds) Bioremediation of industrial waste for environmental safety. Springer, Singapore, pp 265–290. https://doi.org/10.1007/978-981-13-1891-7_13

Nachin L, Nannmark U, Nyström T (2005) Differential roles of the universal stress proteins of Escherichia coli in oxidative stress resistance, adhesion, and motility. J Bacteriol 187(18):6265–6272. https://doi.org/10.1128/JB.187.18.6265-6272.2005

Nicolopoulou-Stamati P, Maipas S, Kotampasi C, Stamatis P, Hens L (2016) Chemical pesticides and human health: the urgent need for a new concept in agriculture. Front Public Health 4:148. https://doi.org/10.3389/fpubh.2016.00148

Nikaido E, Shirosaka I, Yamaguchi A, Nishino K (2011) Regulation of the AcrAB multidrug efflux pump in Salmonella enterica serovar Typhimurium in response to indole and paraquat. Microbiology 157(3):648–655. https://doi.org/10.1099/mic.0.045757-0

Nunn CM, Djordjevic S, Hillas PJ, Nishida CR, de Montellano PRO (2002) The crystal structure of Mycobacterium tuberculosis alkylhydroperoxidase AhpD, a potential target for antitubercular drug design. J Biol Chem 277(22):20033–20040. https://doi.org/10.1074/jbc.M200864200

Ogata H, Goto S, Sato K, Fujibuchi W, Bono H, Kanehisa M (1999) KEGG: Kyoto encyclopedia of genes and genomes. Nucleic Acids Res 27(1):29–34. https://doi.org/10.1093/nar/27.1.29

Okoli UA, Nubila NI, Okafor MT (2017) Organophosphorus pesticide: an environmental pollutant perspective. J Chem Pharm Res 9(9):126–130

Osman D, Cavet JS (2010) Bacterial metal-sensing proteins exemplified by ArsR–SmtB family repressors. Nat Prod Rep 27(5):668–680. https://doi.org/10.1039/B906682A

Paget MS, Helmann JD (2003) The σ 70 family of sigma factors. Genome Biol 4(1):203. https://doi.org/10.1186/gb-2003-4-1-203

Pailan S, Sengupta K, Saha P (2020) Microbial metabolism of organophosphates: key for developing smart bioremediation process of next generation. In: Arora PK (ed) Microbial Technology for Health and Environment. Springer, Singapore, pp 361–410. https://doi.org/10.1007/978-981-15-2679-4_14

Pakala SB, Gorla P, Pinjari AB, Krovidi RK, Baru R, Yanamandra M, Merrick M, Siddavattam D (2007) Biodegradation of methyl parathion and p-nitrophenol: evidence for the presence of a p-nitrophenol 2-hydroxylase in a Gram-negative *Serratia* sp. strain DS001. Appl Microbiol Biotechnol 73(6):1452–1462. https://doi.org/10.1007/s00253-006-0595-z

Phan G, Benabdelhak H, Lascombe MB, Benas P, Rety S, Picard M, Ducruix A, Etchebest C, Broutin I (2010) Structural and dynamical insights into the opening mechanism of P. aeruginosa OprM channel. Structure 18(4):507–517. https://doi.org/10.1016/j.str.2010.01.018

Poirier L, Jacquet P, Plener L, Masson P, Daudé D, Chabrière E (2018) Organophosphorus poisoning in animals and enzymatic antidotes. Environ Sci Pollut Res. https://doi.org/10.1007/s11356-018-2465-5

Popoca-Ursino EC, Martínez-Ocampo F, Dantán-González E, Sánchez-Salinas E, Ortiz-Hernández ML (2017) Characterization of methyl parathion degradation by a *Burkholderia zhejiangensis* strain, CEIB S4-3, isolated from agricultural soils. Biodegradation 28(5-6):351–367. https://doi.org/10.1007/s10532-017-9801-1

Schroeder A, Mueller O, Stocker S, Salowsky R, Leiber M, Gassmann M, Lightfoot S, Menzel W, Granzow M, Ragg T (2006) The RIN: an RNA integrity number for assigning integrity values to RNA measurements. BMC Mol Biol 7(1):3. https://doi.org/10.1186/1471-2199-7-3

Sharma RK, Singh P, Setia A, Sharma AK (2020) Insecticides and ovarian functions. Environ Mol Mutagen 61(3):369–392. https://doi.org/10.1002/em.22355

Shen W, Liu W, Zhang J, Tao J, Deng H, Cao H, Cui Z (2010) Cloning and characterization of a gene cluster involved in the catabolism of p-nitrophenol from *Pseudomonas putida* DLL-E4. Bioresour Technol 101(19):7516–7522. https://doi.org/10.1016/j.biortech.2010.04.052

Siddavattam D, Khajamohiddin S, Manavathi B, Pakala SB, Merrick M (2003) Transposon-like organization of the plasmid-borne organophosphate degradation (opd) gene cluster found in *Flavobacterium* sp. Appl Environ Microbiol 69(5):2533–2539. https://doi.org/10.1128/AEM.69.5.2533-2539.2003

Siddiqa A, Islam MJ, Rahman MS, Uddin MN, Fancy R (2016) Assessing toxicity of organophosphorus insecticide on local fish species of Bangladesh. Int J Fish Aquat Stud 4:670–676

Spain JC, Gibson DT (1991) Pathway for biodegradation of p-nitrophenol in a Moraxella sp. Appl Environ Microbiol 57(3):812–819

Stanley J, Preetha G (2016) Pesticide toxicity to microorganisms: exposure, toxicity and risk assessment methodologies. In: Pesticide toxicity to non-target organisms. Springer, Dordrecht. https://doi.org/10.1007/978-94-017-7752-0_6

Subashchandrabose SR, Megharaj M, Venkateswarlu K, Naidu R (2012) p-Nitrophenol toxicity to and its removal by three select soil isolates of microalgae: the role of antioxidants. Environ Toxicol Chem 31(9):1980–1988. https://doi.org/10.1002/etc.1931

Symmons MF, Bokma E, Koronakis E, Hughes C, Koronakis V (2009) The assembled structure of a complete tripartite bacterial multidrug efflux pump. Proc Natl Acad Sci 106(17):7173–7178. https://doi.org/10.1073/pnas.0900693106

Takeo M, Murakami M, Niihara S, Yamamoto K, Nishimura M, Kato DI, Negoro S (2008) Mechanism of 4-nitrophenol oxidation in Rhodococcus sp. strain PN1: characterization of the two-component 4-nitrophenol hydroxylase and regulation of its expression. J Bacteriol 190(22):7367–7374. https://doi.org/10.1128/JB.00742-08

Takeshita K, Shibata TF, Nikoh N, Nishiyama T, Hasebe M, Fukatsu T, Shigenobu S, Kikuchi Y (2014) Whole-genome sequence of Burkholderia sp. strain RPE67, a bacterial gut symbiont of the bean bug *Riptortus pedestris*. Genome Announc 2(3):e00556–e00514. https://doi.org/10.1128/genomeA.00556-14

Thorvaldsdóttir H, Robinson JT, Mesirov JP (2013) Integrative genomics viewer (IGV): high-performance genomics data visualization and exploration. Brief Bioinform 14(2):178–192. https://doi.org/10.1093/bib/bbs017

Tiwari B, Verma E, Chakraborty S, Srivastava AK, Mishra AK (2018) Tolerance strategies in cyanobacterium Fischerella sp. under pesticide stress and possible role of a carbohydrate-binding protein in the metabolism of methyl parathion (MP). Int Biodeterior Biodegradation 127:217–226. https://doi.org/10.1016/j.ibiod.2017.11.025

Upadhayay J, Rana M, Juyal V, Bisht SS, Joshi R (2020) Impact of pesticide exposure and associated health effects. In: Srivastava PK, Singh VP, Singh A, Tripathi DK, Singh S, Prasad SM, Chauhan DK (eds) Pesticides in crop production: physiological and biochemical action. John Wiley and Sons Ltd., Hoboken, pp 69–88. https://doi.org/10.1002/9781119432241.ch5

Urióstegui-Acosta M, Tello-Mora P, Solís-Heredia MJ, Ortega-Olvera JM, Piña-Guzmán B, Martín-Tapia D, González-Mariscal L, Quintanilla-Vega B (2020) Methyl parathion causes genetic damage in sperm and disrupts the permeability of the blood-testis barrier by an oxidant mechanism in mice. Toxicology 438:152463. https://doi.org/10.1016/j.tox.2020.152463

Vikram S, Pandey J, Bhalla N, Pandey G, Ghosh A, Khan F, Jain RK, Raghava GP (2012) Branching of the p-nitrophenol (PNP) degradation pathway in Burkholderia sp. strain SJ98: evidences from genetic characterization of PNP gene cluster. AMB Express 2(1):30. https://doi.org/10.1186/2191-0855-2-30

Vikram S, Pandey J, Kumar S, Raghava GPS (2013) Genes involved in degradation of para-nitrophenol are differentially arranged in form of non-contiguous gene clusters in *Burkholderia* sp. strain SJ98. PLoS One 8(12):1–13. https://doi.org/10.1371/journal.pone.0084766

Vollmer AC, Bark SJ (2018) Twenty-five years of investigating the universal stress protein: function, structure, and applications. In: Sariaslani S, Gadd GM (eds) Advances in Applied Microbiology. Academic Press, United States, pp 1–36. https://doi.org/10.1016/bs.aambs.2017.10.001

Wei Q, Liu H, Zhang JJ, Wang SH, Xiao Y, Zhou, NY (2010) Characterization of a para-nitrophenol catabolic cluster in Pseudomonas sp. strain NyZ402 and construction of an engineered strain capable of simultaneously mineralizing both para-and ortho-nitrophenols. Biodegradation 21(4):575–584. https://doi.org/10.1007/s10532-009-9325-4

Zar JH (2010) Biostatistical analysis, 5th edn. Prentice Hall, New Jersey, p 944

Zhang J, Sun Z, Li Y, Peng X, Li W, Yan Y (2009a) Biodegradation of p-nitrophenol by *Rhodococcus* sp. CN6 with high cell surface hydrophobicity. J Hazard Mater 163(2-3):723–728. https://doi.org/10.1016/j.jhazmat.2008.07.018

Zhang JJ, Liu H, Xiao Y, Zhang XE, Zhou NY (2009b) Identification and characterization of catabolic para-nitrophenol 4-monooxygenase and para-benzoquinone reductase from *Pseudomonas* sp. strain WBC-3. J Bacteriol 191(18):2703–2710. https://doi.org/10.1128/JB.01566-08

Zhang S, Sun W, Xu L, Zheng X, Chu X, Tian J, Wu N, Fan, Y (2012) Identification of the para-nitrophenol catabolic pathway, and characterization of three enzymes involved in the hydroquinone pathway, in Pseudomonas sp. 1-7. BMC Microbiol 12(1):1–11. https://doi.org/10.1186/1471-2180-12-27

Zhang X, Yang YS, Lu Y, Wen YJ, Li PP, Zhang G (2018) Bioaugmented soil aquifer treatment for P-nitrophenol removal in wastewater unique for cold regions. Water Res 144:616–627. https://doi.org/10.1016/j.watres.2018.08.004

Zheng Y, Liu D, Liu S, Xu S, Yuan Y, Xiong L (2009) Kinetics and mechanisms of p-nitrophenol biodegradation by *Pseudomonas aeruginosa* HS-D38. J Environ Sci 21(9):1194–1199. https://doi.org/10.1016/S1001-0742(08)62403-1

Zhongli C, Shunpeng L, Guoping F (2001) Isolation of methyl parathion-degrading strain M6 and cloning of the methyl parathion hydrolase gene. Appl Environ Microbiol 67(10):4922–4925

Zomot E, Yardeni EH, Vargiu AV, Tam HK, Malloci G, Ramaswamy VK, Perach M, Ruggerone P, Pos KM, Bibi E (2018) A new critical conformational determinant of multidrug efflux by an MFS transporter. J Mol Biol 430(9):1368–1385. https://doi.org/10.1016/j.jmb.2018.02.026